Journal of Integrative Agriculture 2026, 25(8): 3400–3411

Available online at ScienceDirect

Journal of Integrative Agriculture



RESEARCH ARTICLE

Isopropoxy benzene guanidine: A promising new weapon against enterococcal infections

Jianxin Hu[1], Yongxiang Zhang[1], Jinyu Yang[1], Sujuan Wu[1], Weiqi Liu[1], Yixing Lu[1,2], Wenguang Xiong[1], Dongping Zeng[1], Zhenling Zeng[1#]

[1] *College of Veterinary Medicine, South China Agricultural University/Guangdong Provincial Key Laboratory of Veterinary Pharmaceutics Development and Safety Evaluation/National Risk Assessment Laboratory for Antimicrobial Resistance of Animal Original Bacteria, Guangzhou 510642, China*
[2] *Zhaoqing Academy of Agricultural and Forestry Sciences, Zhaoqing 526000, China*

Highlights

- Isopropoxy benzene guanidine (IBG) kills a wide range of enterococci.
- IBG disrupts bacterial cell membranes.
- IBG cures skin infections caused by enterococci.

Abstract

The emergence of antibiotic resistance represents a significant threat to human health. Human activities have accelerated the development of antibiotic resistance, underscoring the urgent need to develop novel antibiotics in addressing the challenge of antibiotic-resistant bacteria. Isopropoxy benzene guanidine (IBG) is a substituted benzyl guanidine derivative with good antibacterial activity against enterococci. In this study, the antibacterial activity of IBG against enterococci derived from dogs, cats, and pigs was evaluated (with a minimal inhibitory concentration range of 1–16 μg mL^{-1}) and the epidemiological cut-off values (ECOFFs) were determined using ECOFFinder. The ECOFFs for *Enterococcus faecalis* and *Enterococcus faecium* were both 16 μg mL^{-1}. The drug resistance development results showed that IBG has a low bacterial resistance risk. The antibacterial mechanism studies showed that IBG disrupts bacterial cell membranes by interacting with phosphatidylglycerol or cardiolipin. IBG inhibits the formation of *E. faecalis* biofilms, but it cannot eradicate them. The results of the *Galleria mellonella* larvae infection model and mouse dermal infection model suggested that IBG has therapeutic effects on enterococcal infections *in vivo*. In conclusion, IBG appears to be a good candidate for the treatment of enterococcal infections.

Keywords: enterococci, isopropoxy benzene guanidine, antibacterial activity, antibacterial mechanism

1. Introduction

Enterococcus spp. are prevalent bacteria in the intestinal flora of humans and animals. Some *Enterococcus* strains without transferable antibiotic resistance and virulence genes can be used as probiotics to improve the balance of the gastrointestinal microbiota in animals. However, with an imbalance in the symbiotic state between the host and the enterococci, some enterococci from the normal intestinal tract may enter other tissues and organs and cause infections (Agudelo Higuita and Huycke 2014). Enterococci play a decisive role in mixed infections with multiple microorganisms. They can promote multiple microbial infections that lead to more complex pathogenesis and poorer prognosis, which reduces the efficacy of antibiotics by promoting the colonization, proliferation, and persistence of multiple pathogenic organisms, thereby posing a serious threat to human health (Xu *et al.* 2024). In China, the rate of vancomycin resistance in *Enterococcus faecium* was 1.7% in 2022, representing a 0.5% increase relative to 2021. *Enterococcus faecalis* resistance remained at 0.2% (CARSS 2023). In 2022, the average rate of resistance to vancomycin among *E. faecium* isolates in EU countries also showed an

Received 4 September 2024; Received in revised form 14 November 2024; Accepted 2 December 2024; Available online 24 December 2024
Jianxin Hu, E-mail: 986651198@qq.com; #Correspondence Zhenling Zeng, E-mail: zlzeng@scau.edu.cn

© 2026 CAAS. Publishing services by Elsevier B.V. on behalf of KeAi Communications Co. Ltd. This is an open access article under the CC BY-NC-ND license (http://creativecommons.org/licenses/by-nc-nd/4.0/). Peer review under responsibility of Editorial Board of *Journal of Integrative Agriculture*.
doi: 10.1016/j.jia.2024.12.026

increasing trend year on year, from 16.2% in 2018 to 17.6% in 2022 (ECFDP 2023).

Antibiotic resistance has become a global concern and major public health challenge, and the development of new antibiotics is essential for addressing this challenge (Laxminarayan *et al.* 2013; Jesudason 2024). Guanidine-containing compounds have antibacterial, antifungal, antitumor, and antiviral activities (Wang *et al.* 2014; Pasero *et al.* 2018; Ciarlantini *et al.* 2021; Liang *et al.* 2021). These compounds can exert their bactericidal effect by altering cell membrane permeability and targeting phospholipids, thereby disrupting the cytoplasmatic membrane (Gomes *et al.* 2023). Robenidine is an anticoccidial agent used to prevent chicken coccidiosis (Kantor *et al.* 1970). Studies have subsequently demonstrated that these compounds exhibit antibacterial activity, both in their native form and in their derivatives (Abraham *et al.* 2016; Ogunniyi *et al.* 2017). Isopropoxy benzene guanidine (IBG) belongs to the group of substituted benzyl guanidine derivatives, and it has a structure very similar to robenidine. *In vitro* and *in vivo* studies on the effective antibacterial activity of IBG against Gram-negative (*Riemerella anatipestifer*) and Gram-positive (*Staphylococcus aureus*, *Streptococcus suis*, and *Clostridium perfringens*) bacteria have been reported (Zhang *et al.* 2021; Lu *et al.* 2022, 2024; Han *et al.* 2023). IBG can also be employed as an antibacterial synergist. In *R. anatipestifer*, the combination of IBG and gentamicin is synergistic (Lu *et al.* 2024). In *S. aureus*, IBG is synergistic with kanamycin (Li *et al.* 2023). In *Escherichia coli* and *Salmonella*, IBG was also found to be synergistic with colistin (Kong *et al.* 2022; Li *et al.* 2023). The main metabolic pathway of IBG in rat liver microsomes is hydroxylation, which generates seven metabolites (Lu *et al.* 2023). IBG has an acceptable safety profile with an oral LD_{50} of about 1,800 mg kg^{-1} in rats. A sperm deformity test in mice showed that IBG does not have reproductive genotoxicity in mice, and the results of a teratogenicity test in rats showed that IBG is not embryotoxic or teratogenic in rats (Peng 2019).

Previous studies suggested that IBG also has antibacterial activity against *E. faecalis* and *E. faecium* (Zhang *et al.* 2019). In this study, the activity of IBG against enterococci was further tested, and the time-killing curves of IBG against *E. faecalis* and *E. faecium* were plotted. ECOFFinder was used to establish the epidemiological cut-off values (ECOFFs) of IBG against *E. faecalis* and *E. faecium*. Using fluorogenic probes, the alterations in bacterial physiology after the impact of IBG on enterococci were further elucidated, thereby providing further insight into the disruptive effects of IBG on the membrane. The influence of membrane phospholipid components on the minimal inhibitory concentration (MIC) of IBG was further investigated through exogenous addition. These findings suggested that IBG exerts bactericidal activity against enterococci by rupturing the bacterial cell membrane through its interaction with phosphatidylglycerol (PG) or cardiolipin (CL). The effectiveness of commonly used antibiotics in combination with IBG was evaluated to expand the scope of IBG applications. The impact of IBG on biofilm formation in *E. faecalis* was investigated. In addition, the *in vivo* antibacterial activity of IBG was evaluated using *Galleria mellonella* larvae and mouse dermal infection models.

2. Materials and methods

2.1. Materials

A total of 565 enterococcal strains were used in this study, including *E. faecalis* ATCC29212 and *E. faecium* ATCC19434. Both brain heart infusion (BHI) broth and agar and Mueller-Hinton (MH) broth and agar were used for the culture of enterococci. IBG (98%) were synthesized by Guangzhou Insighter Biotechnology (Guangzhou, China). PG, CL, and phosphatidylethanolamine (PE) were purchased from Sigma-Aldrich (Saint Louis, Missouri, USA). Crystal violet solution, florfenicol (FFC), rifampicin (RIF), enrofloxacin (ENR), linezolid (LZD), tedizolid (TZD), doxycycline (DOX), gentamicin (GEN), erythromycin (ERY), clindamycin (CLI), vancomycin (VAN), ceftiofur (CEF), penicillin (PEN), and amoxicillin (AMO) were purchased from Yuan Ye (Shanghai, China). Propidium iodide (PI), the BCECF-AM fluorescent probe, ROS Assay Kit, and BCA Protein Assay Kit were purchased from Beyotime (Shanghai, China), and DiSC3(5) was obtained from MedChemExpress (MCE; Monmouth Junction, New Jersey, USA).

2.2. Determination of the MIC

According to the Clinical and Laboratory Standards Institute Guidelines (Clinical and Laboratory Standards Institute 2020), the agar dilution method was used to determine the MICs of antibiotics (including IBG) against enterococci. After incubation at 37°C for 16–18 h, the MIC values of antibiotics that inhibit bacterial growth were observed and recorded. The quality control strain was *E. faecalis* ATCC29212.

2.3. Establishment of ECOFFs for IBG by *E. faecalis* and *E. faecium*

ECOFFs were determined using ECOFFinder, and the ECOFFs with confidence intervals of 95% were taken (Turnidge *et al.* 2006). The ECOFF represents the upper limit of the range of MIC values for wild-type strains. Therefore, strains with MIC values less than or equal to this ECOFF are classified as wild-type strains, while strains with MIC values greater than this ECOFF are considered non-wild-type strains. The resistance rate is the proportion of the number of non-wild-type strains to the total number of strains tested.

2.4. Time-killing curves

The time-killing curves of IBG against *E. faecalis* and *E. faecium* were determined. Overnight cultures of enterococci were diluted at a ratio of 1:100 and treated with 0–16 μg mL^{-1} IBG. The colony counts were obtained by continuous dilution and plate counting.

2.5. Assay for the inhibition and eradication of biofilms

A diluted bacterial solution was added to IBG, and the final concentration of IBG was 0–2 μg mL^{-1}. After incubation at 37°C for 24 h, the culture was discarded, and the well was washed with phosphate buffered saline (PBS) three times and dried, stained with 0.1% crystal violet solution for 15 min, and then washed with water three times. After drying at 60°C for 15 min, 50 μL of anhydrous ethanol was

added to each well to fully dissolve the crystal violet, and the optical density (OD) value was measured at 595 nm. Similarly, the steps for the biofilm eradication assay were as follows. First, 200 μL of bacterial suspension was added to each well of a 96-well plate and incubated at 37°C for 48 h. Then, the culture was discarded, the residue was washed with PBS three times, then BHI broth containing a final concentration of 40–120 μg mL^{-1} IBG was added and the solution was incubated for 12 h. Biofilms were also detected by the crystal violet staining method. One-way ANOVA was used for the statistical analysis (*, P<0.05; **, P<0.01; ***, P<0.001).

2.6. Drug resistance development

The potential of *E. faecalis* and *E. faecium* to develop drug resistance to IBG was assessed as previously described (Lu *et al.* 2024), with the exception that MH broth was used as the culture medium in this study.

2.7. Antibacterial mechanism

Membrane depolarization assay Changes in membrane potential (ΔΨ) were detected using a DiSC3(5) fluorescent probe. The bacterial solution was washed with buffer A (5 mmol L^{-1} HEPES and 20 mmol L^{-1} glucose) and then the $OD_{600\ nm}$ was adjusted to 0.5 with buffer B (5 mmol L^{-1} HEPES, 20 mmol L^{-1} glucose, and 100 mmol L^{-1} KCl). The probe was added and the solution was incubated for 30 min at 37°C while shielded from light. The bacterial solution and IBG were added to the black 96-well plate to give final IBG concentrations in the range of 0–32 μg mL^{-1}. The change in fluorescence intensity was monitored over 1 h using a multimode microplate reader, with an excitation wavelength of 622 nm and an emission wavelength of 670 nm.

ΔpH assay Intracellular pH was determined using the BCECF-AM fluorescent probe as previously described (Han *et al.* 2023). The bacterial solution was washed with PBS and the $OD_{600\ nm}$ was adjusted to 0.5. After adding the probe, the solution was incubated at 37°C in the dark for 30 min. The bacterial solution and IBG were added to a black 96-well plate with final IBG concentrations in the range of 0–32 μg mL^{-1}. Following an incubation period of 1 h at 37°C, the fluorescence intensity was quantified using an excitation wavelength of 488 nm and an emission wavelength of 535 nm.

Membrane permeability assay Membrane permeability was assessed using a PI fluorescent probe based on a previously described method (Han *et al.* 2023). The bacterial solution was washed with PBS and the $OD_{600\ nm}$ was adjusted to 0.5. The probe was added followed by incubation in the dark at 37°C for 30 min. The bacterial solution and IBG were added to a black 96-well plate, achieving final IBG concentrations in the range of 0–32 μg mL^{-1}. Subsequently, the fluorescence intensity was quantified following a one-hour static incubation at 37°C (excitation wavelength: 535 nm, emission wavelength: 615 nm).

ROS determination The intracellular detection of ROS was achieved using a ROS Assay Kit (Beyotime, Shanghai, China). After washing the bacterial solution with PBS, the $OD_{600\ nm}$ was adjusted to 0.5. The DCFH-DA probe was added followed by incubation for 30 min at 37°C in the dark. The bacterial solution containing the probe was subjected to a further washing step with PBS to remove any residual probe. Then the bacterial solution and IBG were added to a black 96-well plate, with final IBG concentrations in the range of 0–32 μg mL^{-1}. Changes in fluorescence intensity were monitored over 2 h. The excitation and emission wavelengths were 488 and 525 nm, respectively.

Intracellular content leakage The leakage of intracellular contents was detected at $OD_{260\ nm}$ (Huang *et al.* 2023). IBG was added to the PBS suspensions of *E. faecalis* and *E. faecium* to give final concentrations in the range of 0–32 μg mL^{-1}. The mixture was incubated at 37°C for 2 h followed by centrifugation at 3,500 r min^{-1} for 5 min. The supernatant was aspirated and the leakage of intracellular DNA was detected at 260 nm. The protein concentration was measured using the BCA Protein Concentration Assay Kit (Beyotime, Shanghai, China). After centrifugation, 20 μL of the supernatant was combined with 200 μL of BCA reagent and incubated at 37°C for 30 min. The OD value was then measured at 562 nm.

Data analysis The above experiments were tested for significant differences using one-way ANOVA.

Antibacterial activity of the exogenous additives The effects of PG, CL, and PE on the activity of IBG against *E. faecalis* and *E. faecium* were evaluated by a checkerboard broth dilution assay.

2.8. Antibacterial combination susceptibility testing

The synergistic effects of combining IBG with different antibiotics were determined using the checkerboard broth dilution method, and the specific experimental method and calculation of FICI were conducted according to a previous study (Kong *et al.* 2022). The mechanisms of action of these antibiotics include effects on nucleic acid synthesis (enrofloxacin), cell wall synthesis (ceftiofur, penicillin, amoxicillin, and vancomycin), and protein synthesis (linezolid, tedizolid, doxycycline, gentamicin, erythromycin, florfenicol, and clindamycin).

2.9. *Galleria mellonella* larvae model with infection by *E. faecalis* and *E. faecium*

After overnight culture in BHI broth, the bacteria were collected by centrifugation, washed twice with PBS, and adjusted to the appropriate bacterial density (1.9×10^{8} CFU mL^{-1}). The different forelimbs of *G. mellonella* larvae were injected with 10 μL of bacterial solution and a drug solution using a 0.3 mL insulin syringe (Thieme *et al.* 2020). The positive control group was only injected with bacterial solution, and the negative control group was only injected with PBS. The experimental larvae were divided into three groups, and each treatment group contained 10 *G. mellonella* larvae. The *G. mellonella* larvae were incubated at 37°C for 5 d, and the number of daily *G. mellonella* larval deaths was recorded. Origin software was used to analyze the data, and the Kaplan-Meier survival curve was used to draw the survival map. Statistical analysis was performed using the Mantel-Cox test to compare the survival curves between the PBS control group and each treatment group (*, P<0.05).

2.10. Mouse model of dermal infection with *E. faecalis* or *E. faecium*

Five-wk-old SPF-grade male ICR mice weighing approximately 22 g were acclimatized and fed for 4 d in a negative-pressure animal room. Adequate food and drinking water were provided throughout the trial period. Mice were weighed and randomly divided into six groups: Control (wound without bacterial infection), PBS, IBG-16, IBG-32, IBG-64, and VAN-32. The backs of the mice were shaved and depilated separately using a razor and depilatory cream. After local anesthesia with lidocaine hydrochloride drops on the back, skin incisions were made using a 6 mm diameter skin remover and surgical scissors. All groups except the Control group were infected with the bacterial solution. After 1 d, the remaining groups, except for the Control group, were treated with PBS, IBG, or VAN. The treatments were carried out for 10 d (20 μL once a day) and changes in body weight and wound area were recorded. After the euthanasia of the mice, skin tissue was taken for bacterial collection, and skin slices were made for hematoxylin and eosin (H&E) staining.

3. Results

3.1. Antibacterial activity of IBG against *Enterococcus* spp.

The chemical structure and morphology of IBG are shown in Fig. 1-A. IBG exhibits excellent antibacterial activity against nine species of enterococci, including *E. faecium*, with an MIC_{50} of 4 μg mL^{-1} (Table 1). The distribution of IBG MIC values for *E. faecalis* and *E. faecium* from different animal sources varied (Fig. 1-B and C). The distribution of IBG MIC values for *E. faecalis* and *E. faecium* isolated from pigs and cats ranged from 4 to 8 μg mL^{-1} and 1 to 16 μg mL^{-1}, respectively. The MIC values of dog-derived *E. faecium* were distributed in the range of 2–8 μg mL^{-1}, while those of *E. faecalis* for IBG were in the range of 1–16 μg mL^{-1}.

3.2. ECOFFs and resistance rate

A histogram of the distribution of the raw MIC data and a trend line (circle) was plotted by inputting the data into ECOFFinder. The cumulative distribution was fitted using non-linear regression analysis, resulting in a fitted curve (diamond), and the fitted curve showed a typical single-peaked distribution. The ECOFF value for IBG was 16 μg mL^{-1} for both *E. faecalis* (Fig. 1-D) and *E. faecium* (Fig. 1-E) at a 95% confidence level. The resistance rate of IBG in the isolated enterococci was calculated to be zero.

3.3. Evaluation of bactericidal kinetics

To further validate the bactericidal properties of IBG against *E. faecalis* and *E. faecium*, time-killing kinetic assays were performed at different concentrations (Fig. 1-G–L). In the presence of 4×MIC IBG, the number of *E. faecalis* colonies was reduced by approximately 5.7–7.7 logarithmic values in 8–10 h, and *E. faecium* was reduced by approximately 4.6–6.7 logarithmic values in 12 h compared to the control group. However, higher concentrations of IBG were required to completely kill the bacteria.

3.4. Inhibition of *E. faecalis* biofilms

Enterococci can form biofilms to help them survive in extreme environments and participate in persistent bacterial infections. *Enterococcus faecalis* is more likely to produce biofilms than *E. faecium*. Co-culture of bacteria with sub-inhibitory concentrations of IBG showed that IBG can inhibit biofilm formation in *E. faecalis* ATCC29212 and GD22P70 (Fig. 1-F).

3.5. Antibacterial mechanism of IBG against *E. faecalis* and *E. faecium*

In both *E. faecalis* and *E. faecium*, the membrane depolarization assay results showed the fluorescence intensity was significantly greater in the treated group than the untreated group (Fig. 2-A and B). The higher the concentration of IBG, the stronger the fluorescence intensity of DiSC3(5) and the higher the degree of induced cell membrane depolarization. Meanwhile, the results of the ΔpH assay demonstrated that all fluorescence intensities tended to decrease with an increasing drug concentration, indicating a reduction in intracellular pH (Fig. 2-C and D). Moreover, the data show that an elevated concentration of IBG resulted in a more pronounced disruption of the cell membrane, accompanied by a notable increase in the fluorescence intensity of PI (Fig. 2-E and F). Furthermore, the addition of IBG caused the bacteria to produce more ROS (Fig. 2-G and H) and resulted in the leakage of intracellular contents, including protein (Fig. 2-I–L). These results suggest that disruption of the bacterial cell membrane is followed by greater ROS production and the leakage of intracellular contents, which in turn accelerates bacterial death. More detailed results of the significance analyses are provided in Appendix A.

To further illustrate the membrane-targeting mechanism of IBG, the impact of several additives on the antibacterial activity of IBG was examined by the exogenous addition of PG, PE, and CL. The addition of PG at a concentration greater than or equal to 16 μg mL^{-1} resulted in a more than 8-fold increase in the MIC of *E. faecium* ATCC19434 for IBG. Similarly, the addition of CL at a concentration greater than or equal to 64 μg mL^{-1} resulted in a significant increase in the MIC of *E. faecalis* ATCC29212 for IBG, with an increase of more than 8-fold observed (Table 2). These results indicated that the damaging effect of IBG on bacterial cell membranes may be attributed to its interaction with either PG or CL.

3.6. Combined antibiotic sensitivity results

The fractional inhibitory concentration (FIC) values of IBG in combination with the selected antibiotics were greater than 0.5 but less than or equal to 2, indicating that the combination effects were either additive or neutral. Antibiotics with synergistic anti-enterococcal effects in combination with IBG were not found in this study. The combination results indicated that *E. faecalis* favors an additive effect, whereas *E. faecium* favors a neutral effect (Fig. 3-A). Notably, the probability of an additive effect was higher when IBG was combined with antibiotics that act on cell wall-related issues (Fig. 3-B and C).

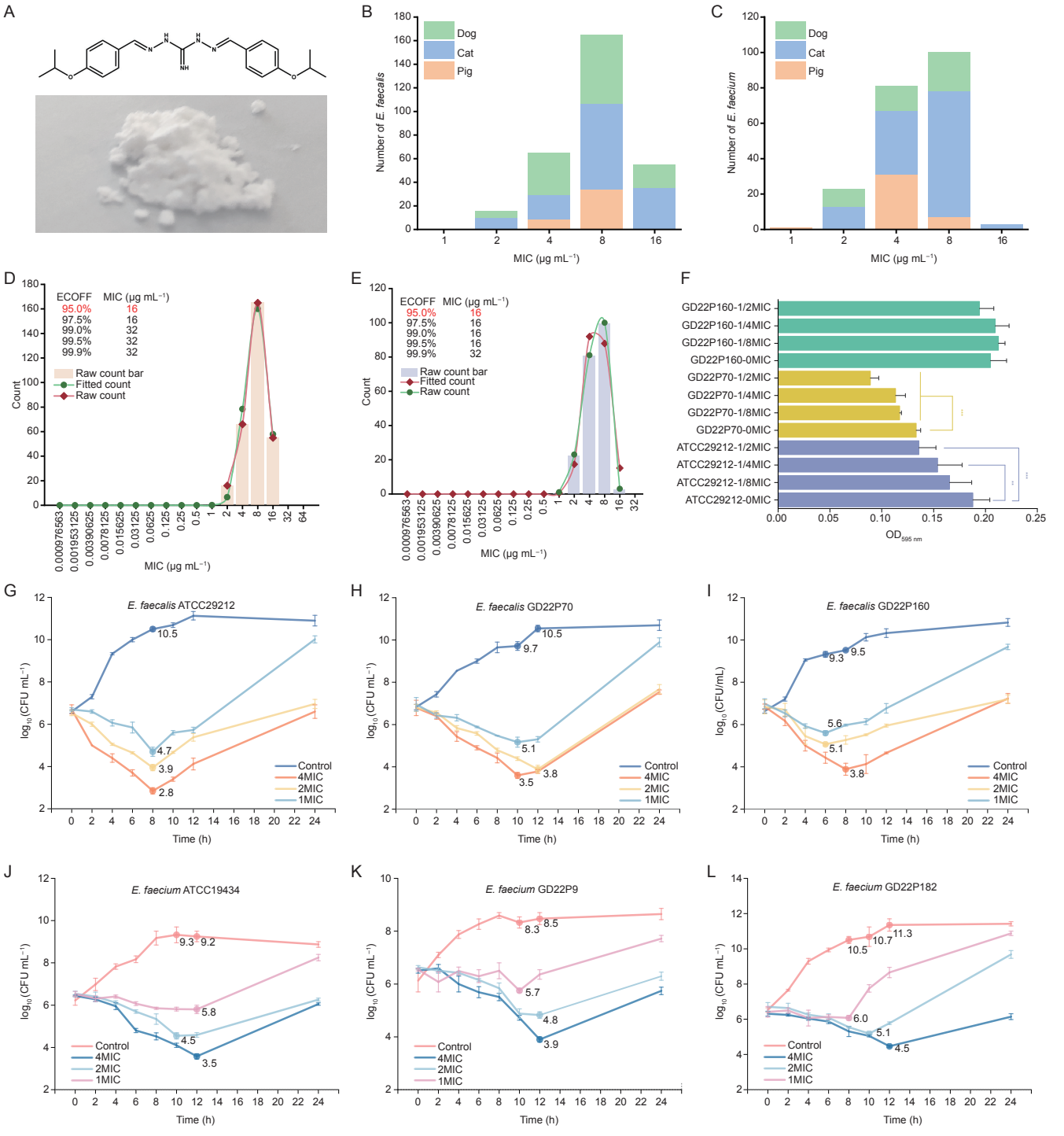


Fig. 1 Anti-enterococcal activity of isopropoxy benzene guanidine (IBG). A, chemical structure and morphology of IBG. B and C, distribution of minimal inhibitory concentration (MIC) values of *Enterococcus faecalis* and *E. faecium* against IBG. D and E, nonlinear regression of the MIC distribution of IBG for *E. faecalis* and *E. faecium*. F, IBG inhibits the formation of *E. faecalis* biofilms. G–I, time-killing curves of IBG against *E. faecalis* ATCC29212, GD22P70 and GD22P160. The MICs against IBG were all 4 μg mL^{-1}. J–L, time-killing curves of IBG against *E. faecium* ATCC19434, GD22P9 and GD22P182. The MICs for IBG were all 2 μg mL^{-1}.

3.7. IBG significantly improved the survival of enterococci-infected *G. mellonella* larvae

IBG at a concentration of 32 μg mL^{-1} significantly increased the survival rate of larvae infected by *optrA*-positive and negative *E. faecalis* and *E. faecium* (P<0.05) (Fig. 3-D-G). Therefore, IBG exerts anti-*E. faecalis* and *E. faecium* activities in treating infections caused by oxazolidinone-resistant bacteria.

3.8. Therapeutic efficacy of IBG in the mouse dermal infection model

The wound area gradually decreased in all groups over

Table 1 Distribution of minimal inhibitory concentration (MIC) values and their MIC_{50} and MIC_{90} levels for isopropoxy benzene guanidine (IBG) in enterococci

Species	Number of strains	MIC (μg mL^{-1})[1)]					MIC_{50} (μg mL^{-1})	MIC_{90} (μg mL^{-1})
		1	2	4	8	16		
Enterococcus faecalis	302	0 (0.0)	16 (5.3)	66 (21.9)	165 (54.6)	55 (18.2)	8	16
E. faecium	208	1 (0.5)	23 (11.1)	81 (38.9)	130 (48.1)	3 (1.4)	4	8
E. hirae	31	0 (0.0)	0 (0.0)	0 (0.0)	31 (100.0)	0 (0.0)	8	8
E. durans	8	0 (0.0)	0 (0.0)	0 (0.0)	8 (100.0)	0 (0.0)	8	8
E. canis	4	0 (0.0)	0 (0.0)	0 (0.0)	4 (100.0)	0 (0.0)	8	8
E. thailandicus	3	0 (0.0)	0 (0.0)	0 (0.0)	3 (100.0)	0 (0.0)	8	8
E. avium	3	0 (0.0)	0 (0.0)	0 (0.0)	3 (100.0)	0 (0.0)	8	8
E. gallinarum	2	0 (0.0)	0 (0.0)	0 (0.0)	2 (100.0)	0 (0.0)	8	8
E. mundtii	2	0 (0.0)	0 (0.0)	0 (0.0)	2 (100.0)	0 (0.0)	8	8

[1)] N (%): N, number of strains; %, percentage of strains in each category relative to the total.

time (Fig. 4-A and C). By d 10, the relative wound areas were significantly different from that of PBS in all groups except for the IBG-16 group (Fig. 4-D). H&E staining showed localized thickening of the stratum corneum and epidermis of the skin tissue in all groups except the Control group, and hemorrhagic foci were seen in the PBS group (Fig. 4-B). Bacteria colony counting results showed that IBG at concentrations of 16, 32, and 64 μg mL^{-1} significantly killed bacteria at the wound site, and IBG was more effective than vancomycin at a concentration of 32 μg mL^{-1} (Fig. 4-E). The relative body weight curves demonstrated no significantly negative impact on the growth of mice (Fig. 4-F). IBG also had a therapeutic effect on skin infections caused by *E. faecium*, since the relative wound areas of both the IBG-16 and IBG-64 groups were significantly different from those of the PBS group on d 10 (P<0.05) (Fig. 5-A, C and D). The results of the H&E staining demonstrated the presence of conspicuous hemorrhagic foci in all groups, except for the Control and IBG-64 groups. In addition, all experimental groups showed localized epidermal thickening (Fig. 5-B). Bacterial enumeration results showed that vancomycin at a concentration of 32 μg mL^{-1} was not as bactericidal as IBG at the same concentration (Fig. 5-E). Similarly, neither IBG nor vancomycin impacted the growth of the mice (Fig. 5-F).

4. Discussion

The ECOFFs for IBG of *E. faecalis* and *E. faecium* were established in this study. The establishment of ECOFF values lays the foundation for future monitoring of antibiotic resistance, screening of resistant strains, and research on the mechanism of antibiotic resistance. The calculated resistance rate can roughly reflect the degree of susceptibility of the enterococci to IBG. The results showed that all isolated enterococcal strains are sensitive to IBG, suggesting that the antibacterial activity of IBG against enterococci is strong.

4.1. IBG reduces the formation of *E. faecalis* biofilm

Biofilms are groups of cells growing on a surface that are surrounded by a polymeric substance matrix, including polysaccharides, proteins, lipids, and extracellular DNA (Flemming and Wingender 2010). Bacteria are more resistant to antibiotics and host immune responses when protected by a biofilm, and the transmission of genetic material through contact is enhanced (Conwell *et al.* 2022). One study analyzed transcriptome differences related to the differences in growth between *E. faecium* in its planktonic and biofilm phases and showed that biofilms may be conducive to horizontal gene transfer (Lim *et al.* 2017). However, the reports of pharmacological small molecules that have both good anti-enterococcal activity (low MIC values) and the ability to inhibit biofilm formation are limited. Solithromycin is a new fourth-generation macrolide antibiotic with MIC values less than or equal to 4 and 8 μg mL^{-1} against *E. faecalis* and *E. faecium*, respectively. This antibiotic inhibited the formation of *E. faecalis* biofilm but did not eradicate it (Wang *et al.* 2021). Telithromycin is a semi-synthetic derivative of erythromycin that has been approved by the US Food and Drug Administration (FDA) for the treatment of community-acquired pneumonia (CAP), acute exacerbation of chronic bronchitis (AECB) and acute maxillary sinusitis (AMS) in adults (Nguyen and Chung 2005). The MIC_{50} values of telithromycin against *E. faecalis* and *E. faecium* were 2 and 4 μg mL^{-1}, respectively, and the MIC_{90} was 8 μg mL^{-1}. Subinhibitory concentrations of telithromycin could also inhibit *E. faecalis* biofilm formation, whereas, in combination with ampicillin, it reduced but did not eradicate mature biofilms (Xiong *et al.* 2021). In this study, IBG could inhibit biofilm formation in *E. faecalis*, but it was unable to effectively eradicate established biofilms. IBG inhibited early biofilm formation, but more detailed experiments with more strains are still needed to further explore the mechanism.

4.2. Induction of IBG resistance in bacteria is difficult

The assessment of antibiotic resistance is an important issue in the design and development of new antibiotics. In this study, the trend of *E. faecalis* and *E. faecium* resistance to IBG was tested, and no resistance developed in 28 days of induction. Previous studies have also evaluated the trend of IBG resistance in *R. anatipestifer*, *S. aureus*, and *S. suis*. No stable IBG-resistant strains were obtained in any of the 28-d resistance induction experiments. In contrast, studies on the induction of resistance to ciprofloxacin produced resistant strains with 256-fold, 512-fold, and 1,024-fold higher MICs for ciprofloxacin against *R. anatipestifer*, *S. aureus*, and *S. suis*, respectively (Han *et al.* 2023; Li *et al.* 2023; Lu *et al.* 2024). This characteristic of difficult resistance induction may be related to the rapid destruction of bacterial cell membranes by the antibiotic (Raheem and Straus 2019).

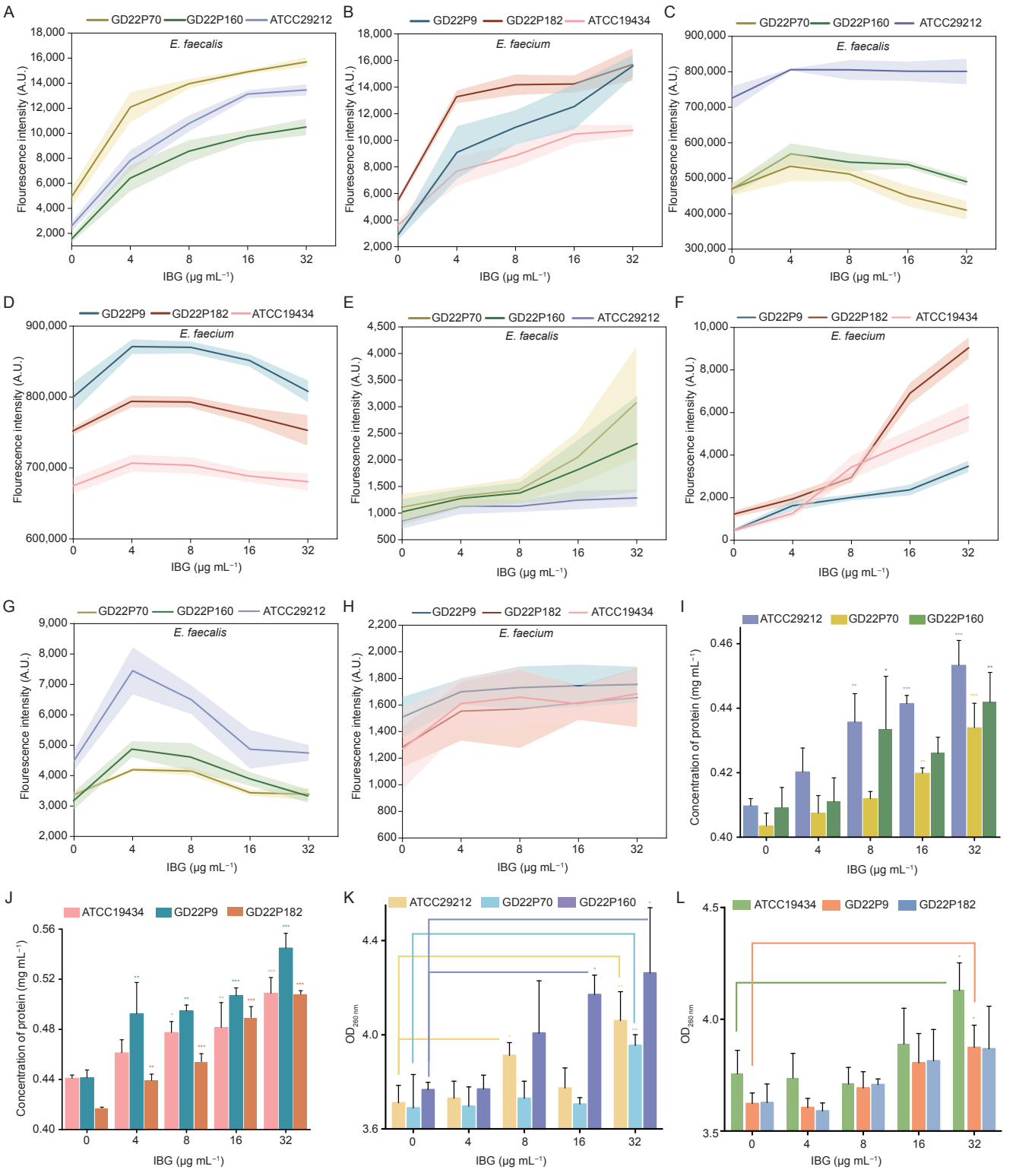


Fig. 2 Bactericidal mechanism of isopropoxy benzene guanidine (IBG). A and B, membrane depolarization measured using a DiSC3(5) fluorescent probe. C and D, intracellular pH detected using the BCECF-AM fluorescent probe. E and F, membrane permeability detected using a PI fluorescent probe. G and H, intracellular ROS changes after the action of IBG on *Enterococcus faecalis* and *E. faecium*. I and J, protein leakage caused by the action of IBG on *E. faecalis* and *E. faecium*. *, **, and *** indicate the results for that group in comparison with the 0 μg mL^{-1} group. K and L, intracellular content leakage resulting from the action of IBG on *E. faecalis* and *E. faecium*.

4.3. IBG destroys cell membranes to kill bacteria

The bacterial proton motive force (PMF) is an energy pathway located in the bacterial membrane. It regulates several biological processes, including ATP synthesis, the active transport of molecules, and the rotation of the bacterial flagella (Yang *et al.* 2023). The two components of the PMF are

Table 2 Fold change in the minimal inhibitory concentrations (MICs) of isopropoxy benzene guanidine (IBG) by the exogenous addition of different phospholipid components

PE (μg mL^{-1})	*Enterococcus faecalis* ATCC29212	*E. faecium* ATCC19434	PG (μg mL^{-1})	*E. faecalis* ATCC29212	*E. faecium* ATCC19434	CL (μg mL^{-1})	*E. faecalis* ATCC29212	*E. faecium* ATCC19434
0	1	1	0	1	1	0	1	1
2	1	1	2	1	1	2	1	1
4	1	1	4	1	1	4	1	1
8	1	1	8	1	1	8	2	1
16	1	1	16	2	>8	16	2	2
32	1	1	32	2	>8	32	4	2
64	1	1	64	4	>8	64	>8	4
128	1	1	128	4	>8	128	>8	>8

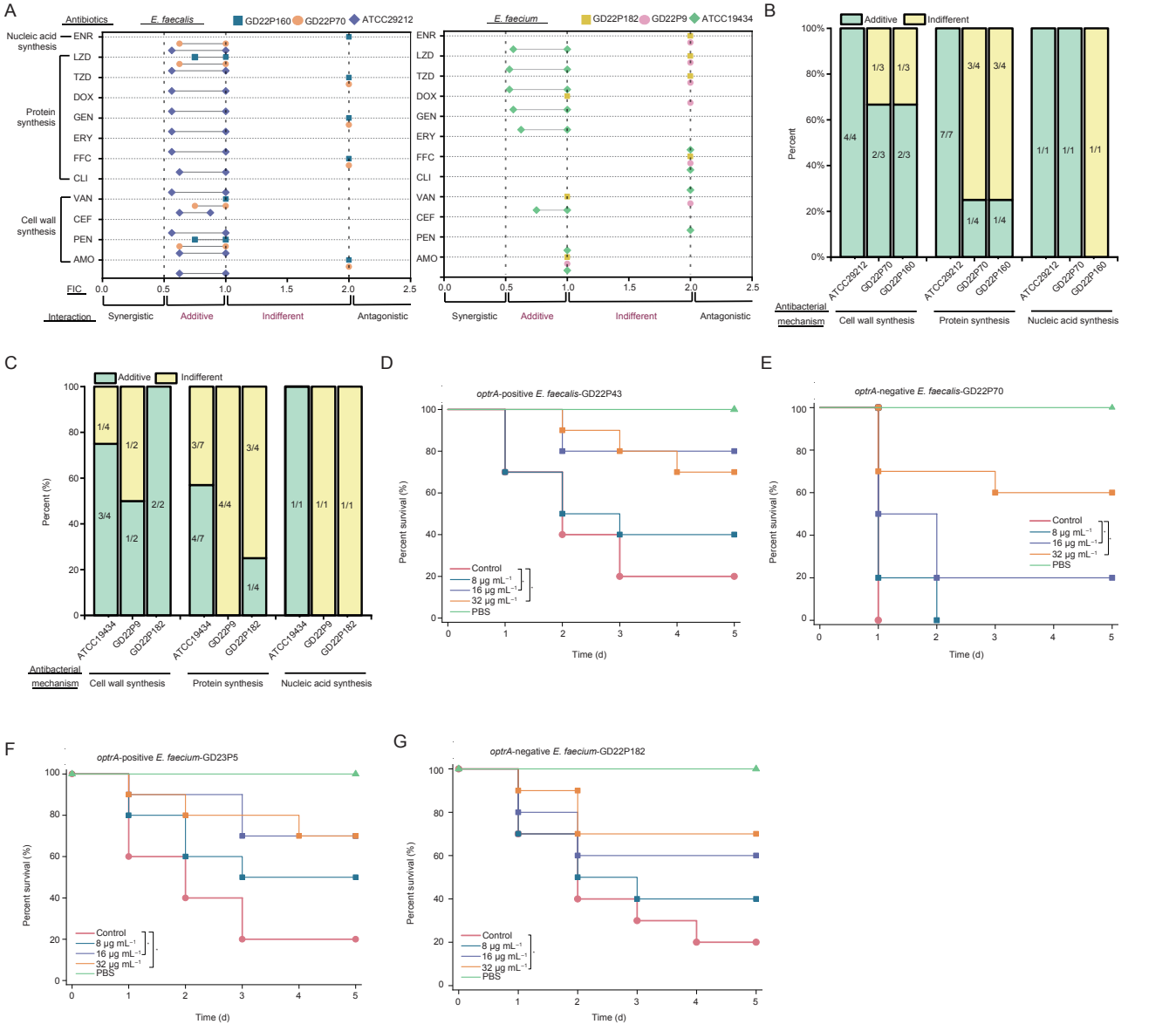


Fig. 3 Results of the checkerboard and survival rate of *Galleria mellonella* larvae. A, results of isopropoxy benzene guanidine (IBG) in combination with commonly used antibiotics in *Enterococcus faecalis* and *E. faecium*. A stock solution of the antibiotic at a higher concentration could not be formulated. Combined antibiotic sensitivity tests could not be performed for these antibiotics (i.e., penicillin (PEN), erythromycin (ERY), gentamicin (GEN), ceftiofur (CEF), and clindamycin (CLI) for isolated *E. faecium* strains and erythromycin (ERY), doxycycline (DOX), ceftiofur (CEF), and CLI for isolated *E. faecalis* strains). B and C, proportional effects of antibiotics when combined with IBG in *E. faecalis* and *E. faecium,* respectively. D and E, effects of IBG treatment on the survival of *G. mellonella* larvae infected with *optrA*-positive *E. faecalis* GD22P43 and *optrA*-negative *E. faecalis* GD22P70. F and G, effects of IBG treatment on the survival of *G. mellonella* larvae infected with *optrA*-positive *E. faecium* GD23P5 and *optrA*-negative *E. faecium* GD22P182.

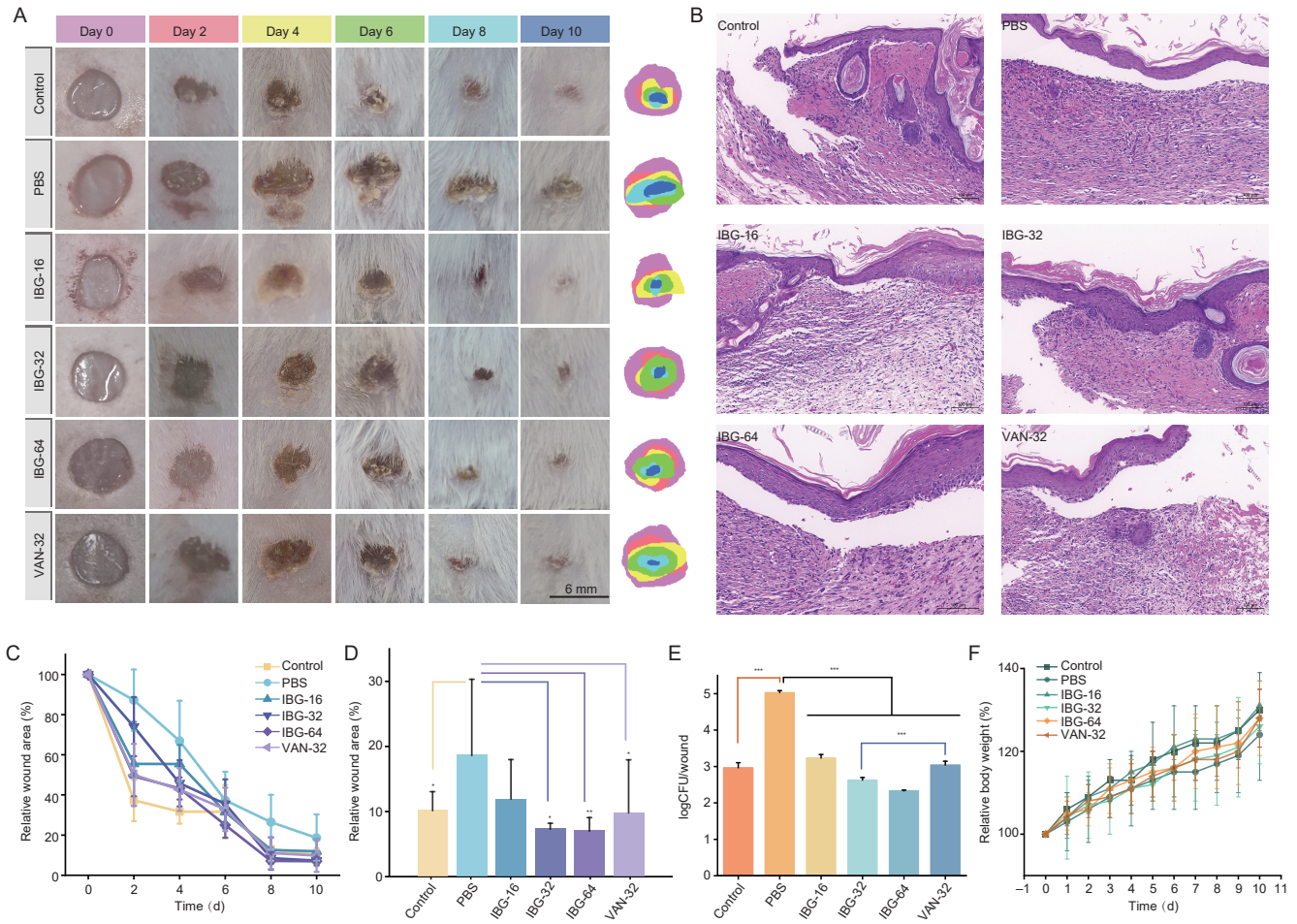


Fig. 4 Efficacy of isopropoxy benzene guanidine (IBG) in a mouse dermal infection model with *Enterococcus faecalis*. *OptrA*-positive *E. faecalis* GD22P43 suspension (10 μL, 4.4×10^{11} CFU mL^{-1}) was added to the wound for infection. The MICs of strain GD22P43 for IBG and vancomycin were 4 and 2 μg mL^{-1}, respectively. A, photographs of the wound site. B, H&E staining images of the skin after the treatments. C, changes in relative wound area from d 0 to d 10 in each group of mice. D, comparison of relative wound areas on d 10 in different groups of mice. E, number of bacteria collected in the wounds of different groups on d 10. F, changes in the body weight of mice after different treatments. Statistical analysis was performed using one-way ANOVA (*, P<0.05; **, P<0.01; ***, P<0.001).

the electrical potential (ΔΨ) and the transmembrane proton gradient (ΔpH) (Chen and Lo 2016). In recent years, many reports have indicated that PMF represents a potential target for antibacterial action. We found that IBG can depolarize the bacterial cell membrane and increase cell membrane permeability in *E. faecalis* and *E. faecium*, which are similar to previous results in *R. anatipestifer*, *S. aureus*, and *S. suis* (Han *et al.* 2023; Li *et al.* 2023; Lu *et al.* 2024). The detection of intracellular ROS showed that IBG induced ROS production. Meanwhile, membrane disruption caused intracellular content leakage, ultimately leading to bacterial death. PG, CL, and PE are three major classes of phospholipids in bacterial cell membranes (Foss *et al.* 2011). The main phospholipid species in Gram-positive bacteria are PG and CL (Epand and Epand 2009), but their relative composition varies from species to species (Joyce and Doran 2023). The relative contents of membrane phospholipids in bacteria are not static and change in response to various environmental conditions. Modifications in phospholipid composition have been shown to influence several crucial cellular processes, including metabolism, stress responses, antibiotic resistance, and virulence (Kuhn *et al.* 2015). The addition of PG and CL had significant effects on the anti-*E. faecalis* and anti-*E. faecium* activities of IBG, which was similar to the results for *R. anatipestifer* and *S. aureus*. In addition, molecular docking results showed that IBG has a high affinity for phosphatidylglycerol phosphate synthase PgsA. The high affinity of PG for IBG has been verified by circular dichroism spectroscopy (Li *et al.* 2023; Lu *et al.* 2024). In recent years, phospholipids have also been reported as antibacterial targets that include small lysine chalcone peptide mimics, coumarin-modified ruthenium complexes, and isoxanthohumol-amine conjugates (Shen *et al.* 2022; Huang *et al.* 2023; Yang *et al.* 2024). These findings suggest that phospholipids in bacterial cell membranes are highly effective as antibacterial drug targets.

4.4. Therapeutic effects of IBG *in vivo*

Galleria mellonella is a suitable model host for studying the efficacy of antibacterial drugs against a range of pathogenic bacteria and may be a viable alternative to traditional mammalian *in vivo* systems (Lebreton *et al.* 2012). The *G. mellonella* larval model of enterococcal infection is a

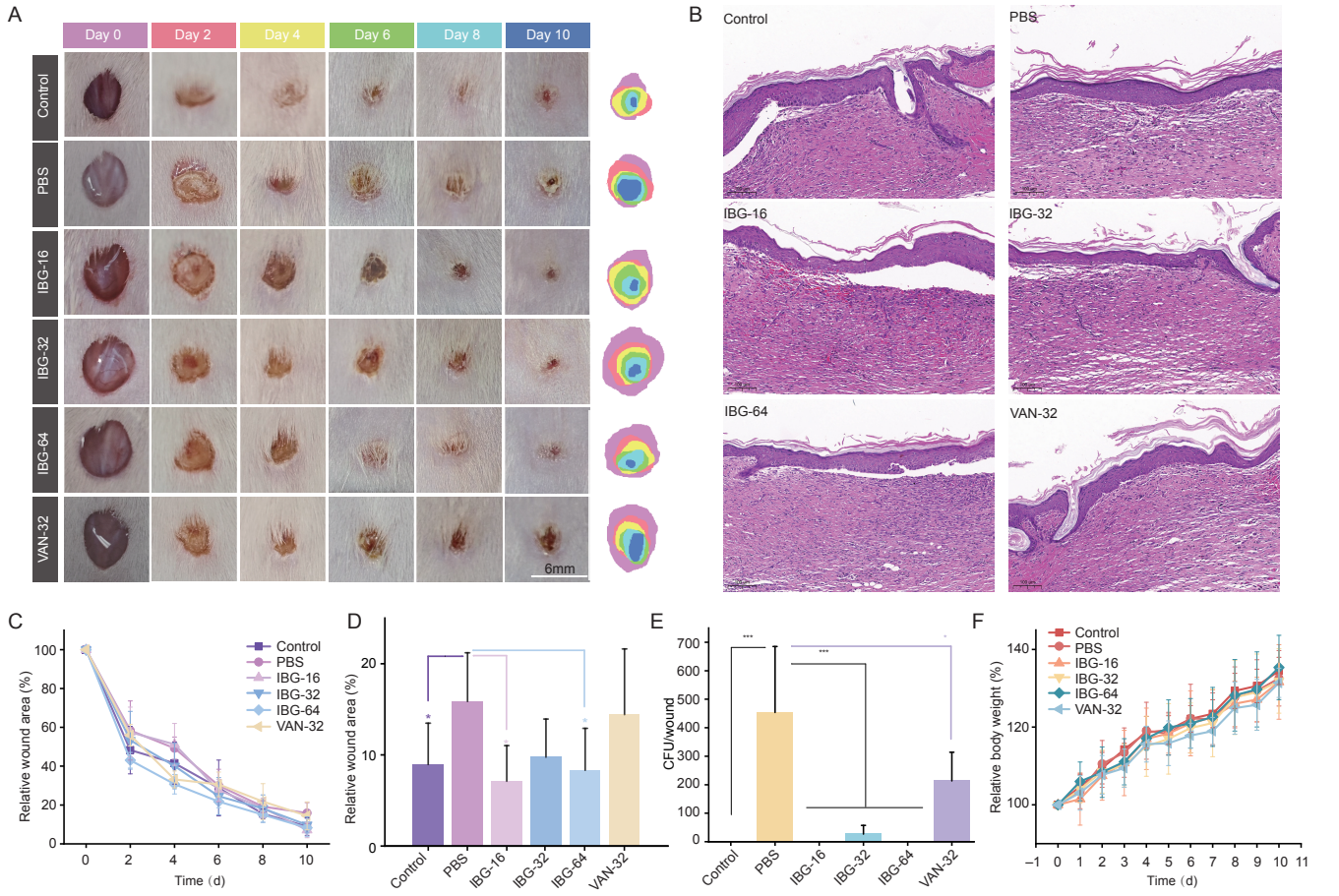


Fig. 5 Efficacy of isopropoxy benzene guanidine (IBG) in a mouse dermal infection model with *Enterococcus faecium*. *OptrA*-positive *E. faecium* GD23P5 suspension (10 μL, 2.6×10^{11} CFU mL^{-1}) was added to the wound for infection. The minimal inhibitory concentrations (MICs) of strain GD23P5 for IBG and vancomycin were both 2 μg mL^{-1}. A, photographs of the wound site. B, results of H&E staining of the skin after treatments. C, changes in relative wound area from d 0 to d 10 for each group of mice. D, comparison of the relative wound areas of mice in each group on d 10. E, number of bacteria collected from the wounds of different groups on d 10. F, impact of various treatments on the body weight of mice. Statistical analysis was performed using one-way ANOVA (*, $P<0.05$; ***, $P<0.001$).

widely applied model for testing the *in vivo* efficacy of new antibacterial drugs, such as microbisporicin (Hofkens *et al.* 2024), and it is also used to assess the synergistic effects of antibacterial drugs *in vivo*, such as ampicillin/ceftriaxone (Thieme *et al.* 2020). This study confirmed that IBG is effective in treating *G. mellonella* infections caused by enterococci.

Gram-positive bacteria, including *Staphylococcus pseudintermedius*, *S. aureus*, *Streptococcus* spp., and *Enterococcus* spp., could be isolated from samples of skin/soft tissue/ear infections in dogs. *Enterococcus* spp. strains were isolated from approximately 5% (71/1409) of these samples (de Jong *et al.* 2020). The most common strain of enterococci isolated from dogs with chronic otitis externa was *E. faecalis* (48.7%), followed by *E. faecium* (21.7%) (Kwon *et al.* 2022). To investigate the therapeutic effect of IBG *in vivo*, a mouse dermal infection model was established. The results showed that IBG was effective in treating skin infections caused by either *E. faecalis* or *E. faecium* and promoted wound healing. To enhance the therapeutic efficacy of IBG, the dosage and number of administrations can be adjusted or the medication can be formulated into more targeted topical preparations, such as creams and sprays.

5. Conclusion

IBG has excellent bactericidal activity both *in vivo* and *in vitro*, and its bactericidal mechanism is closely related to rapid rupture of the membrane. Further modification and development of IBG will be beneficial for the treatment of infections with multi-drug-resistant enterococci.

Acknowledgements

The authors appreciate Dr. Xianfeng Peng from Guangzhou Insighter Biotechnology Co., Ltd., China for providing IBG. This work was supported by the National Natural Science Foundation of China (32273057).

Declaration of competing interest

The authors declare that they have no conflict of interest.

Declaration of generative AI and AI-assisted technologies in the writing process

The authors declare that they did not use AI in the preparation and writing of this manuscript.

Ethical approval

All animal experiments were performed with protocols approved by the Laboratory Animal Center of South China Agricultural University (2024C036).

Appendix associated with this paper is available at https://doi.org/10.1016/j.jia.2024.12.026

References

Abraham R J, Stevens A J, Young K A, Russell C, Qvist A, Khazandi M, Wong H S, Abraham S, Ogunniyi A D, Page S W, O Handley R, Mccluskey A, Trott D J. 2016. Robenidine analogues as Gram-positive antibacterial agents. *Journal of Medicinal Chemistry*, **59**, 2126–2138.

Agudelo Higuita N I, Huycke M M. 2014. Enterococcal disease, epidemiology, and implications for treatment. In: Gilmore M S, Clewell D B, Ike Y, Shankar N, eds. *Enterococci*: *From Commensals to Leading Causes of Drug Resistant Infection*. Massachusetts Eye and Ear Infirmary, Boston.

CARSS (China Antimicrobial Resistance Surveillance System). 2023. Online statistical database: China antimicrobial resistance surveillance for 2022 (Summary version). [2023-11-20]. https://www.carss.cn/Report/Details?aId=917/

Chen M, Lo C. 2016. Using biophysics to monitor the essential protonmotive force in bacteria. In: Leake M C, ed., *Biophysics of Infection*. Springer International Publishing, Cham. pp. 69–79.

Ciarlantini M S, Barquero A, Bayo J, Wetzler D, Dodes T M, Bucci H A, Fiore E J, Gandolfi D L, Defelipe L, Turjanski A, Ramirez J A, Mazzolini G, Comin M J. 2021. Development of an improved guanidine-based rac1 inhibitor with *in vivo* activity against non-small cell lung cancer. *ChemMedChem*, **16**, 1011–1021.

Clinical and Laboratory Standards Institute (CLSI). 2020. *Performance Standards for Antimicrobial Susceptibility Testing*. 30th ed. CLSI supplement M100. Wayne (PA): Clinical and Laboratory Standards Institute, USA.

Conwell M, Dooley J, Naughton P. 2022. Enterococcal biofilm—A nidus for antibiotic resistance transfer?. *Journal of Applied Microbiology*, **132**, 3444–3460.

ECFDP (European Centre for Disease Prevention and Control). 2023. Online statistical database: Antimicrobial resistance in the EU/EEA (EARS-Net)-Annual epidemiological report for 2022. [2023-11-17]. https://www.ecdc.europa.eu/en/publications-data/surveillance-antimicrobial-resistance-europe-2022/

Epand R M, Epand R F. 2009. Domains in bacterial membranes and the action of antimicrobial agents. *Molecular BioSystems*, **5**, 580–587.

Flemming H, Wingender J. 2010. The biofilm matrix. *Nature Reviews Microbiology*, **8**, 623–633.

Foss M H, Eun Y, Weibel D B. 2011. Chemical–biological studies of subcellular organization in bacteria. *Biochemistry*, **50**, 7719–7734.

Gomes A R, Varela C L, Pires A S, Tavares-Da-Silva E J, Roleira F M F. 2023. Synthetic and natural guanidine derivatives as antitumor and antimicrobial agents: A review. *Bioorganic Chemistry*, **138**, 106600.

Han N, Li J, Zhao F, Li Y, Wang J, Dai X, Zeng D, Xiong W, Zeng Z. 2023. Isopropoxy benzene guanidine ameliorates *Streptococcus suis* infection *in vivo* and *in vitro*. *International Journal of Molecular Sciences*, **24**, 7354.

Hofkens N, Gestels Z, Abdellati S, Gabant P, Rodriguez-Villalobos H, Martin A, Kenyon C, Manoharan-Basil S S. 2024. Protective effect of microbisporicin (NAI-107) against vancomycin resistant *Enterococcus faecium* infection in a *Galleria mellonella* model. *Scientific Reports*, **14**, 4786.

Huang H, Wang P, Deng W, Dou L, Liao X, Wang J, Duan X, Yu R, Xiong Y. 2023. Coumarin-modified ruthenium complexes by disrupting bacterial membrane to combat Gram-positive bacterial infection. *Dalton Transactions*, **52**, 9757–9771.

Jesudason T. 2024. WHO publishes updated list of bacterial priority pathogens. *Lancet Microbe*, **5**, 100940.

de Jong A, Youala M, El Garch F, Simjee S, Rose M, Morrissey I, Moyaert H. 2020. Antimicrobial susceptibility monitoring of canine and feline skin and ear pathogens isolated from European veterinary clinics: Results of the ComPath surveillance programme. *Veterinary Dermatology*, **31**, 114–431.

Joyce L R, Doran K S. 2023. Gram-positive bacterial membrane lipids at the host–pathogen interface. *PLoS Pathogens*, **19**, e1011026.

Kantor S, Kennett R L, Waletzky E, Tomcufcik A S. 1970. 1,3-Bis(p-chlorobenzylideneamino) guanidine hydrochloride (Robenzidene): New poultry anticoccidial agent. *Science*, **168**, 373–374.

Kong L, Lu Y, Yang L, Zhang W, Zuo B, Peng X, Qin Z, Li M, Zeng Z, Zeng D. 2022. Pharmacokinetics and pharmacodynamics of colistin combined with isopropoxy benzene guanidine against *mcr-1*-positive *Salmonella* in an intestinal infection Model. *Frontiers in Microbiology*, **13**, 907116.

Kuhn S, Slavetinsky C J, Peschel A. 2015. Synthesis and function of phospholipids in *Staphylococcus aureus*. *International Journal of Medical Microbiology*, **305**, 196–202.

Kwon J, Ko H J, Yang M H, Park C, Park S C. 2022. Antibiotic resistance and species profile of *Enterococcus* species in dogs with chronic otitis externa. *Veterinary Sciences*, **9**, 592.

Laxminarayan R, Duse A, Wattal C, Zaidi A K, Wertheim H F, Sumpradit N, Vlieghe E, Hara G L, Gould I M, Goossens H, Greko C, So A D, Bigdeli M, Tomson G, Woodhouse W, Ombaka E, Peralta A Q, Qamar F N, Mir F, Kariuki S, *et al.* 2013. Antibiotic resistance-the need for global solutions. *Lancet Infectious Diseases*, **13**, 1057–1098.

Lebreton F, Le Bras F, Reffuveille F, Ladjouzi R, Giard J, Leclercq R, Cattoir V. 2012. *Galleria mellonella* as a model for studying *Enterococcus faecium* host persistence. *Journal of Molecular Microbiology and Biotechnology*, **21**, 191–196.

Li J, Zhang X, Han N, Wan P, Zhao F, Xu T, Peng X, Xiong W, Zeng Z. 2023. Mechanism of action of isopropoxy benzene guanidine against multidrug-resistant pathogens. *Microbiology Spectrum*, **11**, e0346922.

Liang P, Shen S, Xu Q, Wang S, Jin S, Lu H, Dong Y, Zhang J. 2021. Design, synthesis biological activity, and docking of novel fluopyram derivatives containing guanidine group. *Bioorganic & Medicinal Chemistry*, **29**, 115846.

Lim S Y, Teh C S J, Thong K L. 2017. Biofilm-related diseases and omics: Global transcriptional profiling of *Enterococcus faecium* reveals different gene expression patterns in the biofilm and planktonic cells. *OMICS*: *A Journal of Integrative Biology*, **21**, 592–602.

Lu Y, Qiao W, Xue Y, Hong X, Jin Y, Li J, Peng X, Zeng D, Zeng Z. 2024. Antibacterial activity of isopropoxy benzene guanidine against *Riemerella anatipestifer*. *Frontiers in Pharmacology*, **15**, 1347250.

Lu Y, Yang L, Zhang W, Li J, Peng X, Qin Z, Zeng Z, Zeng D. 2022. Pharmacokinetics and pharmacodynamics of isopropoxy benzene guanidine against *Clostridium perfringens* in an intestinal infection model. *Frontiers in Veterinary Science*, **9**, 1004248.

Lu Y, Zhang W, Zhang Y, Wu S, Ma M, Peng X, Zeng Z, Zeng D. 2023. Metabolite identification of isopropoxy benzene guanidine in rat liver microsomes by using UHPLC-Q-TOF-MS/MS. *International Journal of Molecular Sciences*, **24**, 7313.

Nguyen M, Chung E P. 2005. Telithromycin: The first ketolide antimicrobial. *Clinical Therapeutics*, **27**, 1144–1163.

Ogunniyi A D, Khazandi M, Stevens A J, Sims S K, Page S W, Garg S, Venter H, Powell A, White K, Petrovski K R, Laven-Law G, Tótoli E G, Salgado H R, Pi H, Coombs G W, Shinabarger D L, Turnidge J D, Paton J C, Mccluskey A, Trott D J, *et al.* 2017. Evaluation of robenidine analog NCL195 as a novel broad-spectrum antibacterial agent. *PLoS ONE*, **12**, e0183457.

Pasero C, D'Agostino I, De Luca F, Zamperini C, Deodato D, Truglio G I, Sannio F, Del P R, Ferraro T, Visaggio D, Mancini A, Guglielmi M B, Visca P, Docquier J D, Botta M. 2018. Alkyl-guanidine compounds as potent broad-spectrum antibacterial agents: Chemical library extension and biological characterization. *Journal of Medicinal Chemistry*, **61**, 9162–9176.

Peng X F. 2019. *Application of Diaminoguanidine Derivatives and Their Feed Compositions in the Preparation of Veterinary Drugs*. China Patent, Application CN201980005962.7. China National Intellectual Property Administration, Beijing, China. (in Chinese)

Raheem N, Straus S K. 2019. Mechanisms of action for antimicrobial peptides with antibacterial and antibiofilm functions. *Frontiers in Microbiology*, **10**, 2866.

Shen B, Wang M, Xu S, Gao C, Wang M, Li S, Ampomah-Wireko M, Chen S, Yan D, Qin S, Zhang E. 2022. Antibacterial efficacy

evaluation and mechanism probe of small lysine chalcone peptide mimics. *European Journal of Medicinal Chemistry*, **244**, 114885.

Thieme L, Hartung A, Makarewicz O, Pletz M W. 2020. *In vivo* synergism of ampicillin, gentamicin, ceftaroline and ceftriaxone against *Enterococcus faecalis* assessed in the *Galleria mellonella* infection model. *Journal of Antimicrobial Chemotherapy*, **75**, 2173–2181.

Turnidge J, Kahlmeter G, Kronvall G. 2006. Statistical characterisation of bacterial wild-type MIC value distributions and the determination of epidemiological cut-off values. *Clinical Microbiology and Infection*, **12**, 418–425.

Wang J, Wang Y, Li Z, Zhan P, Bai R, Pannecouque C, Balzarini J, De Clercq E, Liu X. 2014. Design, synthesis and biological evaluation of substituted guanidine indole derivatives as potential inhibitors of HIV-1 Tat-TAR interaction. *Medicinal Chemistry*, **10**, 738–746.

Wang Y, Xiong Y, Wang Z, Zheng J, Xu G, Deng Q, Wen Z, Yu Z. 2021. Comparison of solithromycin with erythromycin in *Enterococcus faecalis* and *Enterococcus faecium* from China: Antibacterial activity, clonality, resistance mechanism, and inhibition of biofilm formation. *The Journal of Antibiotics*, **74**, 143–151.

Xiong Y, Chen J, Sun X, Xu G, Li P, Deng Q, Yu Z, Chen Z, Zheng J. 2021. The antibacterial and antibiofilm activity of telithromycin against *Enterococcus* spp. isolated from patients in China. *Frontiers in Microbiology*, **11**, 616797.

Xu W, Fang Y, Zhu K. 2024. Enterococci facilitate polymicrobial infections. *Trends in Microbiology*, **32**, 162–177.

Yang B, Tong Z, Shi J, Wang Z, Liu Y. 2023. Bacterial proton motive force as an unprecedented target to control antimicrobial resistance. *Medicinal Research Reviews*, **43**, 1068–1090.

Yang R, Cheng W, Huang M, Xu T, Zhang M, Liu J, Qin S, Guo Y. 2024. Novel membrane-targeting isoxanthohumol-amine conjugates for combating methicillin-resistant *Staphylococcus aureus* (MRSA) infections. *European Journal of Medicinal Chemistry*, **268**, 116274.

Zhang X, Han D, Pei P, Hao J, Lu Y, Wan P, Peng X, Lv W, Xiong W, Zeng Z. 2019. *In vitro* antibacterial activity of isopropoxy benzene guanidine against multidrug-resistant *Enterococci*. *Infection and Drug Resistance*, **12**, 3943–3953.

Zhang X, Xiong W, Peng X, Lu Y, Hao J, Qin Z, Zeng Z. 2021. Isopropoxy benzene guanidine kills *Staphylococcus aureus* without detectable resistance. *Frontiers in Microbiology*, **12**, 633467.

Executive Editor-in-Chief Dongming Zhao
Managing Editor Yanyan Sun